Dynamical effective potentials in electron tunneling: Path-integral study

N. Klipa and M. Šunjić
Department of Physics, University of Zagreb, Bijenička cesta 32, 41000 Zagreb, Croatia
(Received 19 June 1995)

Dynamical effective potential felt by an electron tunneling in the planar metal-insulator-metal system is considered. The tunneling electron coupled to the surface-plasmon modes is described within Feynman's path-integral formalism. Self-consistent numerical results for the effective potentials, tunneling times, and tunneling rates are presented. The classical image potential is obtained in the limit of long tunneling times. It is shown that in cases when the traversal time T becomes comparable to the plasmon, i.e., screening time ω_s^{-1}, considerable departure from the classical image potential appears.

I. INTRODUCTION

In this paper, we consider dynamical effective potential felt by an electron tunneling in a planar metal-insulator-metal (M-I-M) system. Knowledge of this potential is of great importance in determining the current-voltage (I-V) characteristic of an M-I-M heterostructure. In the simplest theoretical approach, a rectangular barrier of height V_0 independent of the distance L between two semi-infinite metals is assumed. It is known that the reduction of the barrier height, due to the image potential has a significant effect on the tunneling resistance.[1,2] In order to improve agreement with experimental results, several attempts were made to find semiempirical corrections to the classical image potential.[1,3] Essential progress was made by realizing that the origin of image potential is in the electron interaction with surface-plasmon (SP) modes.[4,5] Calculation of dynamical corrections to the classical image potential, for an electron moving with uniform velocity perpendicular to the face of a semi-infinite metal, followed.[6–8] Such a semiclassical description is, however, inadequate in a situation where the electron tunnels through the classically forbidden region. Consequently, various quantum-mechanical descriptions of the tunneling electron were presented.[9–12] Experimental evidence for the occurrence of dynamical effects in the limit of short tunneling times[13] gives an additional motivation for further theoretical investigation. More recently,[14–17] a detailed study of the dynamical effective potentials within the Jonson[9] theory was made.

In the present work, tunneling electron coupled to the SP modes is described within the Feynman's path-integral formalism.[18,19] Thus, we avoid the wave function concept, and in contrast to the self-energy approach,[9,10] our treatment is nonperturbative. The paper by Persson and Baratoff[12] is especially relevant for our work, but they have calculated tunneling rates directly, without discussing the image potentials and barrier shapes. We also show that they have underrated the effect of nonlocality, which becomes important for narrow barriers.

We present self-consistent numerical results for the dynamical effective potentials, tunneling times, and tunneling rates for various physical parameters. We show that the classical image potential is obtained in the limit of long tunneling times, and by setting cutoff wave vector q_c of the SP modes to the infinity. In the opposite situation when the traversal time T is comparable with the plasmon, i.e., screening time ω_s^{-1}, the dynamical image potential is obtained. Also, it is pointed out that the effect of nonlocality, which is especially strong for narrow barriers, causes additional reduction of the barrier height.

II. FORMULATION OF THE PROBLEM

For a description of the metallic electrodes, we use the local scalar dielectric function $\epsilon(\omega) = 1 - \omega_p^2/\omega^2$, valid in the long-wavelength limit. Therefore, the electron, which tunnels through the insulator layer ($0 \le z \le L$), is coupled only to the SP modes. For the static barrier described by an arbitrary potential $V(\mathbf{r})$, we write the Hamiltonian[12]

$$H = \frac{\mathbf{p}^2}{2m^*} + V(\mathbf{r}) + \sum_{\mathbf{q},\alpha} \hbar\omega_{\mathbf{q},\alpha} b^\dagger_{\mathbf{q},\alpha} b_{\mathbf{q},\alpha} + \sum_{\mathbf{q},\alpha} \Gamma_{\mathbf{q},\alpha}(z) e^{i\mathbf{q}\cdot\boldsymbol{\rho}} (b_{\mathbf{q},\alpha} + b^\dagger_{-\mathbf{q},\alpha}), \tag{1}$$

where $\mathbf{p}$ and $\mathbf{r} = (z, \boldsymbol{\rho})$ are electron momentum and position operators; $b^\dagger_{\mathbf{q},\alpha}$ and $b_{\mathbf{q},\alpha}$ are the creation and annihilation operators of the SP modes. SP frequencies and coupling matrix elements for even and odd ($\alpha = \pm 1$) plasmon modes, have the form[20,5]

$$\omega_{\mathbf{q},\alpha} = \omega_s \sqrt{1 + \alpha e^{-qL}}, \tag{2}$$

$$\Gamma_{\mathbf{q},\alpha}(z) = \sqrt{\frac{2\pi\hbar\omega_s^2 e^2}{Aq\omega_{\mathbf{q},\alpha}}} \frac{e^{q(z-L)} + \alpha e^{-qz}}{2}, \tag{3}$$

where A is the interface unit area.

Propagator of the system with several degrees of freedom can be represented as a path integral,[18]

$$G(\mathbf{r}^{(f)},\{x^{(f)}_{\mathbf{q},\alpha}\}\ ;\ \mathbf{r}^{(i)},\{x^{(i)}_{\mathbf{q},\alpha}\},-iT) = \int_{\mathbf{r}(0)=\mathbf{r}^{(i)}}^{\mathbf{r}(T)=\mathbf{r}^{(f)}} \mathcal{D}\mathbf{r}(\cdot) \times \left(\prod_{\mathbf{q},\alpha}\int_{x_{\mathbf{q},\alpha}(0)=x^{(i)}_{\mathbf{q},\alpha}}^{x_{\mathbf{q},\alpha}(T)=x^{(f)}_{\mathbf{q},\alpha}} \mathcal{D}x_{\mathbf{q},\alpha}(\cdot)\right) \times e^{-S_E(\mathbf{r}(\cdot),\{x_{\mathbf{q},\alpha}(\cdot)\})/\hbar}, \tag{4}$$

where superscripts (f) and (i) denote final and initial values of the electron $(\mathbf{r})$ and SP $[x_{\mathbf{q},\alpha} = \sqrt{\hbar/2\omega_{\mathbf{q},\alpha}}(b_{\mathbf{q},\alpha} + b^{\dagger}_{-\mathbf{q},\alpha})]$ coordinates. S_E is the "Euclidean" action

$$S_E(\mathbf{r}(\cdot),\{x_{\mathbf{q},\alpha}(\cdot)\}) = \int_0^T dt\left[\frac{m^*}{2}\left(\frac{d\mathbf{r}}{dt}\right)^2 + V(\mathbf{r})\right] + \sum_{\mathbf{q},\alpha}\int_0^T dt\left(\frac{1}{2}\frac{dx_{-\mathbf{q},\alpha}}{dt}\frac{dx_{\mathbf{q},\alpha}}{dt} + \frac{\omega^2_{\mathbf{q},\alpha}}{2}x_{-\mathbf{q},\alpha}x_{\mathbf{q},\alpha} + \sqrt{\frac{2\omega_{\mathbf{q},\alpha}}{\hbar}}\Gamma_{\mathbf{q},\alpha}(z)e^{i\mathbf{q}\cdot\rho}x_{\mathbf{q},\alpha}\right). \tag{5}$$

In the planar M-I-M system, the static barrier depends only on the z coordinate, e.g., $V(z) = V_0 - eV_b z/L$, where V_0 is the height of the rectangular barrier (the band offset) and V_b is the applied voltage. For simplicity, we consider only paths perpendicular to the surface, but it is still impossible to find an analytic solution for the path integral (4). We proceed according to Refs. 21, 22, and define the reduced propagator of the system[23] by

$$K(z^{(f)},z^{(i)},-iT) = \int\prod_{\mathbf{q},\alpha} dx^{(i)}_{\mathbf{q},\alpha}\, G(z^{(f)},\{x^{(i)}_{\mathbf{q},\alpha}\};z^{(i)},\{x^{(i)}_{\mathbf{q},\alpha}\},-iT). \tag{6}$$

Following standard procedures,[21] integration over SP coordinates in Eq. (6) may be carried out exactly,

$$K(z^{(f)},z^{(i)},-iT) = \left(\prod_{\mathbf{q},\alpha}\frac{1}{2\sinh(\omega_{\mathbf{q},\alpha}T/2)}\right) \times \int_{z(0)=z^{(i)}}^{z(T)=z^{(f)}} \mathcal{D}z(\cdot)e^{-S_{\rm eff}(z(\cdot))/\hbar}. \tag{7}$$

Here $S_{\rm eff}$ is the effective Euclidean action,

$$S_{\rm eff}(z(\cdot)) = \int_0^T dt\left[\frac{m^*}{2}\left(\frac{dz}{dt}\right)^2 + V(z)\right] - \frac{1}{2\hbar}\int_0^T dt\int_0^T dt'\sum_{\mathbf{q},\alpha}\frac{\cosh[\omega_{\mathbf{q},\alpha}(|t-t'|-T/2)]}{\sinh(\omega_{\mathbf{q},\alpha}T/2)}\Gamma_{\mathbf{q},\alpha}(z(t))\Gamma_{\mathbf{q},\alpha}(z(t')), \tag{8}$$

from which we deduce the expression for the effective potential,

$$V_{\rm eff}(z) = V(z) - \frac{1}{2\hbar}\int_0^T dt'\sum_{\mathbf{q},\alpha}\frac{\cosh\{\omega_{\mathbf{q},\alpha}[|t(z)-t'|-T/2]\}}{\sinh(\omega_{\mathbf{q},\alpha}T/2)}\Gamma_{\mathbf{q},\alpha}(z)\Gamma_{\mathbf{q},\alpha}(z(t')), \tag{9}$$

which is functional of the path taken by the electron. We see that the effective potential (9) at some point z depends on the value of the coupling matrix elements $\Gamma_{\mathbf{q},\alpha}$ at all other points in the barrier region. Effect of this nonlocality will be discussed in the next section.[24]

Substituting (3) into (9), and replacing

$$\sum_{\mathbf{q},\alpha} \to \sum_{\alpha} A\int\frac{d^2q}{(2\pi)^2}, \tag{10}$$

we find

$$V_{\rm eff}(z) = V(z) - \frac{e^2\omega_s^2}{4}\int_0^T dt'\sum_{\alpha}\int_0^{\infty} dq\frac{\cosh\{\omega_{\mathbf{q},\alpha}[|t(z)-t'|-T/2]\}}{\omega_{\mathbf{q},\alpha}\sinh(\omega_{\mathbf{q},\alpha}T/2)}e^{-qL} \times (\cosh\{q[L-z-z(t')]\} + \alpha\cosh\{q[z-z(t')]\}). \tag{11}$$

Before we discuss the criterion for the choice of the path, which will be used in the calculation of the effective potential (11), let us consider a situation in which $L \to \infty$ and an electron is placed in the vicinity of the left metal electrode. From Eq. (2), we conclude that $\omega_{\mathbf{q},\alpha} \to \omega_s$. Also, it is well known that SP modes decay into single-particle excitations for large $\mathbf{q}$, and we introduce a cutoff wave vector q_c, so the effective potential (11) becomes

$$V_{\rm eff}(z) = V(z) - \frac{e^2\omega_s^2}{8}\int_0^T dt' \sum_\alpha \int_0^{q_c} dq \frac{\cosh\{\omega_s[|t(z)-t'|-T/2]\}}{\omega_s \sinh(\omega_s T/2)} e^{-q[z+z(t')]}. \quad (12)$$

Integration over a wave vector yields

$$V_{\rm eff}(z) = V(z) - \frac{e^2\omega_s}{4}\int_0^T dt' \frac{\cosh\{\omega_s[|t(z)-t'|-T/2]\}}{\sinh(\omega_s T/2)} \frac{1-e^{-q_c[z+z(t')]}}{z+z(t')}. \quad (13)$$

In the high plasmon frequency limit $\omega_s \to \infty$, we could take

$$\frac{\cosh\{\omega_s[|t(z)-t'|-T/2]\}}{\sinh(\omega_s T/2)} \to e^{-\omega_s|t(z)-t'|} \to \frac{2}{\omega_s}\delta[t(z)-t'], \quad (14)$$

and find the static classical result

$$V_{\rm eff}(z) = V(z) - \frac{e^2}{4z}(1-e^{-2q_c z}). \quad (15)$$

At the surface $V_{\rm eff}(0) = V(0) - e^2 q_c/2$. The classical divergence is obtained by setting $q_c \to \infty$.

Standard WKB result for the probability that an electron tunnels through the barrier is

$$D(E) = e^{-2B(E)}. \quad (16)$$

In our approach (generalized WKB approximation), the tunneling exponent B can be calculated along the path of least action (8) for which $z(0) = z^{(i)}$ and $z(T) = z^{(f)}$. Requiring $\delta S_{\rm eff} = 0$ to the first order in δz, we obtain

$$m^* \frac{d^2 z}{dt^2} = \frac{dV(z)}{dz} + \frac{e^2\omega_s^2}{4}\int_0^T dt' \sum_\alpha \int_0^\infty dq q \frac{\cosh[\omega_{\mathbf{q},\alpha}(|t-t'|-T/2)]}{\omega_{\mathbf{q},\alpha}\sinh(\omega_{\mathbf{q},\alpha}T/2)} e^{-qL} \times(\sinh\{q[L-z(t)-z(t')]\} - \alpha \sinh\{q[z(t)-z(t')]\}). \quad (17)$$

Equation (17) describes the classical motion of an electron in the inverted effective potential, and this is the reason why we have introduced imaginary time into propagator (4). Without applied voltage, the height of the static barrier is constant $V(z) = V_0$, so the first term on the right hand side of (17) is equal to zero. We can solve (17) numerically for various values of the time T. From the energy conservation requirement, we find

$$T = \int_{z^{(i)}}^{z^{(f)}} \frac{dz}{\sqrt{2[V_{\rm eff}(z)-E]/m^*}}, \quad (18)$$

which is the traversal time for the particle moving between classical turning points $z^{(i)}$ and $z^{(f)}$ in the inverted effective potential.[25]

We solve the equation (17) by iteration. It is convenient to use the classical motion of the electron in the inverted static barrier for zeroth iteration denoted by $z_{\rm cl}^{(0)}$, with the corresponding traversal time $T^{(0)}$. Now the solution $z_{\rm cl}^{(1)}$ of equation (17) can be used to calculate the first iteration $V_{\rm eff}^{(1)}(z)$ of the effective potential (11). This enables us to solve Eq. (18) for the first iteration of the traversal time $T^{(1)}$. After a few steps, we can thus obtain the self-consistent solutions for $z_{\rm cl}$, $V_{\rm eff}$, and T.

Tunneling exponent B is now given by

$$B = [S_{\rm eff}(z_{\rm cl}) - ET]/\hbar. \quad (19)$$

Note that Eq. (19) is equivalent to the standard expression for the WKB exponent,

$$B = \int_{z^{(i)}}^{z^{(f)}} dz \sqrt{2m^*[V_{\rm eff}(z)-E]/\hbar^2}. \quad (20)$$

III. RESULTS AND DISCUSSION

In this section, we present and discuss self-consistent numerical solutions of Eqs. (17), (18), and (11) for various SP frequencies, electron energies, and barrier widths. In order to avoid divergences in Eqs. (17) and (11) at metallic surfaces, wave vector integration is performed with the cutoff wave vector q_c. As in the $L \to \infty$ case discussed in the previous section, the finite cutoff wave vector affects the barrier only near interfaces. For comparison, in Figs. 1, 2 and 3, the classical image potential[5]

$$V_{\rm cl}(z) = V_0 - \frac{e^2}{4L}[2\Psi(1) - \Psi(z/L) - \Psi(1-z/L)] \quad (21)$$

is drawn, where Ψ is a digamma function.

Figure 1 shows the energy dependence of the dynamical effective potentials $V_{\rm eff}(z)$ for three SP frequencies ($\hbar\omega_s = 0.01, 0.05, 0.2$ Ry). We see that the $V_{\rm eff}(z)$ is not too sensitive on electron energy. As electron energy approaches the top of the barrier, the iteration procedure fails because the traversal time T rapidly increases,

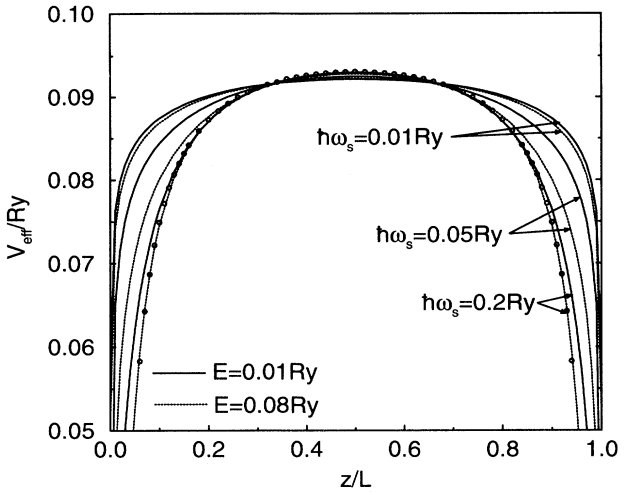

FIG. 1. Dynamical effective potentials for the parameters: potential step $V_0 = 0.1$ Ry, effective mass $m^* = 0.07m$, barrier width $L = 200a_0$. Circles: classical image potential.

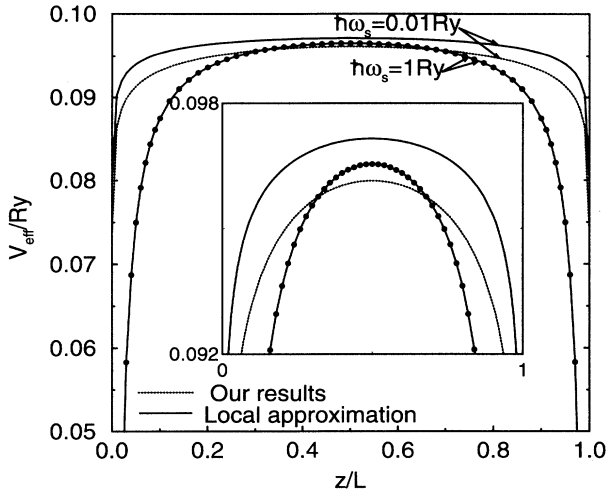

FIG. 3. Same as Fig. 2, but for barrier width $L = 400a_0$. Inset: enlarged top of barriers.

which results in a rapid increase of the right hand side of Eq. (17). So, we take electron energy $E = 0.08$ Ry as an upper bound in our calculation, while $V_0 = 0.1$ Ry. This energy would be enough for the real excitation of SP modes of the frequencies $\hbar\omega_s = 0.01$ Ry and 0.05 Ry. However, because of the small electrode separation in the considered systems, the probability that an electron will traverse the barrier without dissipation is large.[26] The fundamental parameter in our theory is the product $\omega_s T$, which takes the values $0.94, 2.82, 4.79, 18.34, 20.34, 78.67$ for the effective potentials shown in Fig. 1. The smallest value ($\omega_s T = 0.94$, i.e., the traversal time is comparable with the plasmon time) corresponds to $\hbar\omega_s = 0.01$ Ry and $E = 0.01$ Ry, when departure from the classical image potential (21) is strongest. Coincidence with the classical image potential is achieved for $\hbar\omega_s = 0.2$ Ry and $E = 0.08$ Ry, i.e., for $\omega_s T = 78.67$, when the traversal time becomes considerably longer than the plasmon time. This happens exactly when $\omega_s T \to \infty$ (for $q_c \to \infty$), i.e., for a static electron, but in this case there is no tunneling at all.

The WKB tunneling exponent given by Eq. (19) or (20) is shown in Fig. 4. This exponent is calculated up to $\hbar\omega_s = 1$ Ry, in order to show that the classical limit is recovered even for lowest electron energies. Nevertheless, its value is increased about $10 - 30\,\%$, due to dynamical effects. This will have a significant influence on the tunneling rate (16), and consequently on the I-V characteristic of a M-I-M heterostructure.

Figs. 2 and 3 show dynamical effective potentials for narrow ($L = 100a_0$) and wide ($L = 400a_0$) barriers in both dynamic and static (classical) limits. Persson and

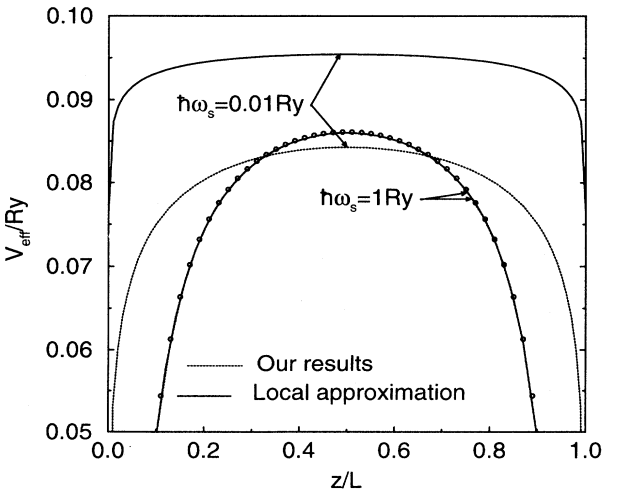

FIG. 2. Dynamical effective potentials for the parameters: potential step $V_0 = 0.1$ Ry, effective mass $m^* = 0.07m$, barrier width $L = 100a_0$, and electron energy $E = 0.05$ Ry. Circles: classical image potential.

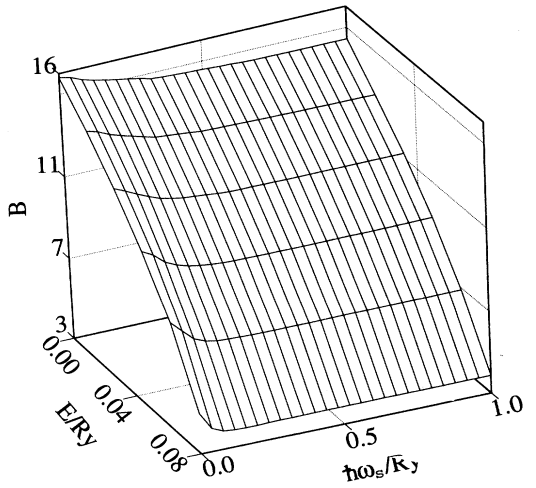

FIG. 4. WKB tunneling exponent for the parameters as in Fig. 1.

Baratoff,[12] following the arguments of Refs. 21, 22, have replaced $\frac{\epsilon\hbar[\omega_{\mathbf{q},\alpha}(|t-t'|-T/2)]}{s\hbar(\omega_{\mathbf{q},\alpha}T/2)}$ with $e^{-\omega_{\mathbf{q},\alpha}|t-t'|}$ in equation (8), which we shall call the "local approximation." In addition to our results, we show in Figs. 2 and 3, dynamical effective potentials calculated in this local approximation. In the high frequency limit, both results tend to the classical image potential. Disagreement arises for low SP frequency and is particularly strong for the narrow barrier shown in Fig. 2. In order to explain such behavior, let us consider for simplicity only the top of the dynamical barrier. Using symmetry in integration over t' when $t' = T/2$, i.e., $z = L/2$, and the fact that $\Gamma_{\mathbf{q},-}(L/2) = 0$, effective potential (9) can be written in the form

$$V_{\text{eff}}(L/2) = V_0 - \frac{1}{\hbar}\int_0^{T/2} dt' \sum_{\mathbf{q}} e^{-\omega_{\mathbf{q},+}(T/2-t')} \times \frac{1+e^{-2\omega_{\mathbf{q},+}t'}}{1-e^{-\omega_{\mathbf{q},+}T}} \Gamma_{\mathbf{q},+}(L/2)\Gamma_{\mathbf{q},+}(z(t')). \quad (22)$$

The term $\frac{1+e^{-2\omega_{\mathbf{q},+}t'}}{1-e^{-\omega_{\mathbf{q},+}T}}$ omitted in the local approximation is responsible for the barrier lowering in our calculations. Without this term, the contribution of the coupling matrix elements $\Gamma_{\mathbf{q},+}(z(t'))$ is attenuated by the factor $e^{-\omega_{\mathbf{q},+}(T/2-t')}$, as $z(t')$ moves towards the metal surface where $\Gamma_{\mathbf{q},+}$ is largest. Including this term, which increases for lower SP frequencies and smaller barrier widths (i.e., traversal times T), this attenuation is suppressed. Therefore, stronger nonlocality is responsible for the reduction of the barrier height below the classical image potential. For a wide barrier shown in Fig. 3, the effect of nonlocality is weak even for the low SP frequency, because traversal time T increases (see Fig. 5), so that the attenuation length becomes small in comparison with the barrier width. Similar conclusions about nonlocality effects have been drawn in Refs. 15–17, where attenuation is contained in the Green's function.[24]

Traversal time (18), as a function of electron energy and barrier width for both dynamic ($\hbar\omega_s = 0.01$ Ry) and static ($\hbar\omega_s = 1$ Ry) limits, is shown in Fig. 5. A remarkable difference is obtained for $E = 0.08$ Ry and $L = 100a_0$, and its origin is obvious from Fig. 2. Namely, traversal distance $z^{(f)} - z^{(i)}$ for the dynamical barrier is greater, and its height is lower than for the classical image potential, so the corresponding traversal time (18) is raised.

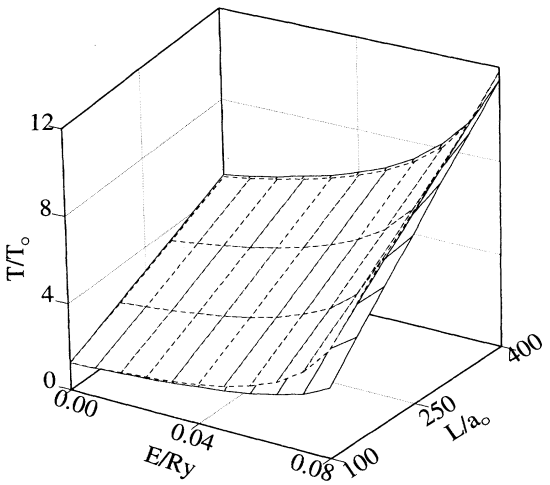

FIG. 5. Traversal time T in units $T_0 = \hbar/V_0$ for the parameters: potential step $V_0 = 0.1$ Ry, effective mass $m^* = 0.07m$. Solid line: $\hbar\omega_s = 1$ Ry; dashed line: $\hbar\omega_s = 0.01$ Ry.

In conclusion, we can say that (i) the dynamical effective potential (9), as defined within the Feynman's path-integral formalism, is not too sensitive on electron energy; (ii) in the cases when traversal time T becomes short enough to be comparable with the plasmon, i.e., screening time ω_s^{-1} dynamical effects appear; (iii) the WKB tunneling exponent is increased about 10 – 30 %, due to dynamical effects; and (iv) the effect of nonlocality is strong, especially for narrow barriers.

[1] J. G. Simmons, in *Tunneling Phenomena in Solids*, edited by Elias Burstein and Stig Lundqvist (Plenum Press, New York, 1969), pp. 135–148.
[2] G. Binnig, N. Garcia, H. Rohrer, J. M. Soler, and F. Flores, Phys. Rev. B **30**, 4816 (1984).
[3] A. Harstein and Z. A. Weinberg, J. Phys. C **11**, L469 (1978); Phys. Rev. B **20**, 1335 (1979).
[4] A. A. Lucas, Phys. Rev. B **4**, 2939 (1971); A. A. Lucas and M. Šunjić, Phys. Lett. **38A**, 413 (1972); J. Vac. Sci. Technol. **9**, 725 (1972); Surf. Sci. **32**, 439 (1972); R. H. Ritchie, Phys. Lett. **38A**, 189 (1972).
[5] Z. Lenac and M. Šunjić, Nuovo Cimento B **33**, 681 (1976).
[6] M. Šunjić, G. Toulouse, and A. A. Lucas, Solid State Commun. **11**, 1629 (1972).
[7] R. Ray and G. D. Mahan, Phys. Lett. **42A**, 301 (1972).
[8] P. M. Echenique, R. H. Ritchie, N. Barberán, and John Inkson, Phys. Rev. B **23**, 6486 (1981).
[9] M. Jonson, Solid State Commun. **33**, 743 (1980).
[10] P. M. Echenique, A. Gras-Marti, J. R. Manson, and R. H. Ritchie, Phys. Rev. B **35**, 7357 (1987); J. R. Manson and R. H. Ritchie, *ibid.* **24**, 4867 (1981).
[11] R. A. Young, Solid State Commun. **45**, 263 (1983).
[12] B. N. J. Persson and A. Baratoff, Phys. Rev. B **38**, 9616 (1988).
[13] P. Guéret, E. Marclay, and H. Meier, Appl. Phys. Lett. **53**, 1617 (1988).
[14] M. Šunjić and L. Marušić, Phys. Rev. B **44**, 9092 (1991).
[15] D. B. Tran Thoai and M. Šunjić, Solid State Commun. **77**, 955 (1991).
[16] M. Šunjić and L. Marušić, Solid State Commun. **84**, 123 (1992).
[17] L. Marušić and M. Šunjić, Solid State Commun. **88**, 781 (1993).
[18] R. P. Feynman and A. R. Hibbs, *Quantum Mechanics and*

Path Integrals (McGraw-Hill, New York, 1965).
[19] L. S. Schulman, *Techniques and Applications of Path Integration* (Wiley, New York, 1981).
[20] M. Šunjić and A. A. Lucas, Phys. Rev. B **3**, 719 (1971).
[21] R. P. Feynman, *Statistical Mechanics* (Benjamin, New York, 1972).
[22] A. O. Caldeira and A. J. Leggett, Ann. Phys. (N.Y.) **149**, 374 (1983).
[23] A somewhat complicated definition for a strictly elastic process is given in Ref. 11.
[24] In Refs. 9 and 14–17 we meet a similar situation. The SP contribution to the effective potential in Eq. (9) is analogous to the expression $\int dz' \phi_{\mathbf{k}}(z')/\phi_{\mathbf{k}}(z) \sum_{\mathbf{q},\alpha} G_{\mathbf{k}-\mathbf{q}}(z,z',E-\hbar\omega_{\mathbf{q},\alpha})\Gamma_{\mathbf{q},\alpha}(z)\Gamma_{\mathbf{q},\alpha}(z')$ in their formalism. Green function and product of the coupling matrix elements at different points arise from the definition of nonlocal self-energy that describes electron-SP interaction.
[25] E. H. Hauge and J. A. Støvneng, Rev. Mod. Phys. **61**, 917 (1989). For the rectangular barrier this is just Larmor time for transmission $\tau_{zT}^{L} \simeq m^* L/\hbar\kappa$.
[26] M. Heiblum, M. I. Nathan, D. C. Thomas, and C. M. Knoedler, Phys. Rev. Lett. **55**, 2200 (1985).